Clinical Study

ASJ Asian Spine J. 2025;19(2): 183-193
https://doi.org/10.31616/asj.2025.0050
PISSN 1976-1902 • eISSN 1976-7846

Special issue

Development and validation of a cost-effective three-dimensional-printed cervical spine model for endoscopic posterior cervical foraminotomy training: a prospective educational study from Turkey

Bilal Bahadır Akbulut[1,2], Elif Ezgi Çenberlitaş[1], Mustafa Serdar Bölük[1], Taşkın Yurtseven[1], Hüseyin Biçeroğlu[1]

[1]Department of Neurosurgery, Ege University, Izmir, Turkey
[2]Department of Biomedical Technologies, Ege University, Izmir, Turkey

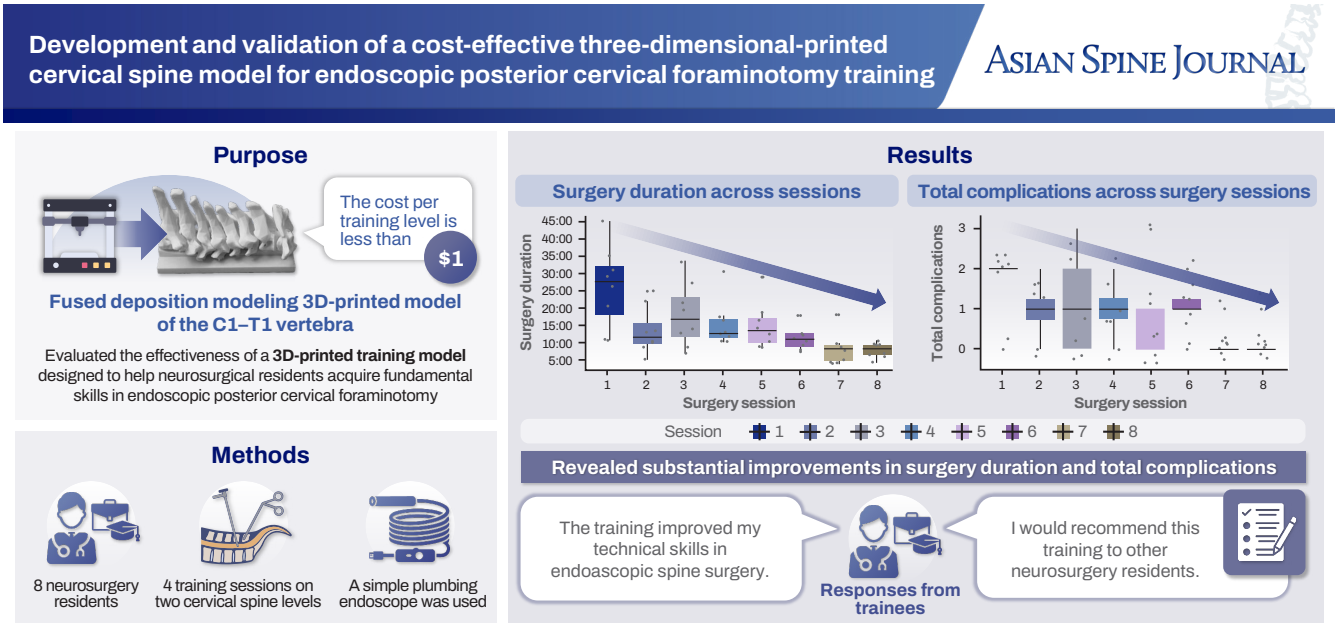

Received Jan 22, 2025; **Revised** Mar 3, 2025; **Accepted** Mar 16, 2025
Corresponding author: Bilal Bahadır Akbulut
Department of Neurosurgery, Ege University, Kazimdirik Mah. Bornova, Izmir, Turkey
Tel: +90-5386416669, **Fax:** +90-2323701330, **E-mail:** bilal.akbulut@saglik.gov.tr

Development and validation of a cost-effective three-dimensional-printed cervical spine model for endoscopic posterior cervical foraminotomy training: a prospective educational study from Turkey

Bilal Bahadır Akbulut[1,2], Elif Ezgi Çenberlitaş[1], Mustafa Serdar Bölük[1], Taşkın Yurtseven[1], Hüseyin Biçeroğlu[1]

Study Design: Expanding upon established surgical simulation methods, we developed a fused deposition modeling three-dimensional (3D)-printed model of the C1–T1 vertebra for posterior cervical foraminotomy training that features silicone-based neural elements, polyurethane foam-based ligaments, and polyethylene terephthalate glycol vertebrae.

Purpose: This study evaluated the effectiveness of a cost-efficient 3D-printed training model designed to help neurosurgical residents acquire fundamental skills in endoscopic posterior cervical foraminotomy while addressing the technique's challenging learning curve and limited training resources.

Overview of Literature: Only a few studies have investigated the efficacy of such a model.

Methods: Eight neurosurgery residents each with over 2 years of training completed four training sessions on two randomly assigned cervical spine levels using the newly developed 3D-printed model. A simple plumbing endoscope was used for real-time surgical visualization.

Results: Among the 64 completed surgical levels, left-sided procedures showed significantly higher insufficient decompression rates than did right-sided procedures (25.0% vs. 3.6%, p=0.002). However, no significant difference in overall complication rates was observed between sides (p=0.073). Surgical parameters remained consistent across sides, with no significant differences in operative duration. Brunner-Langer analysis revealed substantial improvements in operative duration (mean duration decrease from 21:42±2:15 to 6:33±0:42 minutes, p=0.004) and total complications (mean decrease from 2.1±0.8 to 0.4±0.5, p=0.007) across sessions. Although fluoroscopy timing showed marginal improvement (mean duration decrease from 2:12±1:15 to 0:55±0:23 minutes, p=0.057), the number of fluoroscopic images tended to decrease.

Conclusions: Our findings suggest that this novel 3D-printed cervical spine model could be a viable, low-cost option for neurosurgical training programs aiming to help residents develop essential endoscopic skills in a controlled setting. Facilitating early proficiency in posterior cervical foraminotomy can serve as a valuable intermediate step before transitioning to cadaveric models and clinical practice.

Keywords: Endoscopes; Residency; Minimally invasive surgical procedures; Three-dimensional printing; Simulation training

Introduction

Endoscopic posterior cervical foraminotomy has garnered increasing attention as a minimally invasive technique that somewhat reduced infection rates and decreased postoperative pain compared to conventional microsurgical approaches [1-5]. Despite these benefits, the procedure has a shallow learning curve, necessitating substantial hands-on experience to mitigate potential complications, such as root palsy, dural tears, and iatrogenic instability [4,6-10].

Evidently, this outstanding technique requires thorough training, yet access to comprehensive educational resources remains limited, particularly in low- and middle-income countries. Traditional training modalities, including cadaveric dissections and high-end commercial simulators, can be cost prohibitive and are often subject to ethical and logistical barriers [11-13]. These constraints hinder the widespread adoption of endoscopic procedures and impede the democratization of neurosurgical education.

In response, alternatives such as three-dimensional (3D)-printed models and virtual reality (VR) simulators have gained traction given their cost-effectiveness and ease of dissemination [14-20]. Although VR solutions bypass many logistical hurdles, they cannot replicate the tactile feedback inherent to physical training models. In contrast, 3D-printed simulators can be produced inexpensively, with none of the ethical concerns associated with animal or cadaveric use, while still providing hands-on experience in surgical anatomy and instrumentation.

 https://doi.org/10.31616/asj.2025.0050

To address these challenges, we developed a fused deposition modeling (FDM) 3D-printed cervical spine model to help neurosurgery trainees understand the fundamentals of endoscopic posterior cervical foraminotomy. Using readily available materials and a straightforward design, we aimed to create a realistic yet highly affordable model that could serve as an intermediary step before transitioning to more advanced and costly simulation tools. The current study evaluated the effectiveness of our novel simulator in facilitating early skill acquisition among neurosurgery residents.

Materials and Methods

Ethical standards and participant consent

This study adhered to the ethical principles outlined in the Declaration of Helsinki and had received ethical approval from the Institutional Review Board of Ege University (decision no., 24-4.1T/17; date: April 25, 2024), ensuring that all research involving human subjects was conducted following internationally recognized ethical standards. Before participating in the study, informed consent was obtained from all neurosurgery residents.

Vertebra model preparation

Using spine model files licensed under the Creative Commons Attribution-Share Alike 2.1 Japan license [21], we developed a 3D model spanning from C1 to T1. The model incorporates a silicone-based spinal cord and roots, as well as a polyurethane foam expanding foam to simulate soft tissue structures. Meshmixer ver. 35.0 (Autodesk, San Francisco, CA, USA) was used to modify the vertebra and add a baseplate, whereas Autodesk Fusion ver. 2.0.x (Autodesk) was employed to create the mold for the dura, roots, and skin, along with a rigid box to serve as a waterproof container and dark chamber.

The final model was printed on a P1S FDM printer (Bambu Lab, Shenzhen, China) using three walls, a 0.2-mm layer height, 30% adaptive infill, and four top layers. To ensure consistency, all models used in the study were printed according to these specifications. Additional printing details and relevant files are available in our online repository (https://github.com/AkbulutBB/cervicalendoscope).

Soft tissue preparation

A silicone mold was prepared for the spinal cord and nerve roots using Fusion 360 (https://www.autodesk.com/), with a separate mold created for the "skin." This skin features two slit openings where instruments could be introduced, overlying the dark chamber. Room-temperature-vulcanizing silicone with a Shore hardness of 5 was selected for its affordability and suitability in simulating tissue-like properties. Unlike our previous lumbar model wherein the lamina and vertebral body was printed separately [22], the current model was created by printing the C1–T1 vertebrae as a single piece (Fig. 1A). We then threaded the silicone spinal cord through the spinal canal, inserted the roots into their corresponding foramina using forceps (Fig. 1B), and sprayed expanding insulation polyurethane foam to fill the disc space. This foam simulated a protruding disc by pushing the roots posteriorly and then enveloping the roots to mimic the ligamentum flavum. After a 24-hour curing period, any foam that expanded beyond the lamina was trimmed with a snap-blade knife, subsequently exposing the lamina and the facets (Fig. 1C).

Training equipment design and setup

We improved upon our previous lumbar model by introducing a sliding mechanism attached to a plastic tub rather than securing the model with screws into plywood (Fig. 2A, B). This adjustment allowed for more efficient switching between trainees and prevented wear on the attachment plate. Given our budget constraints,

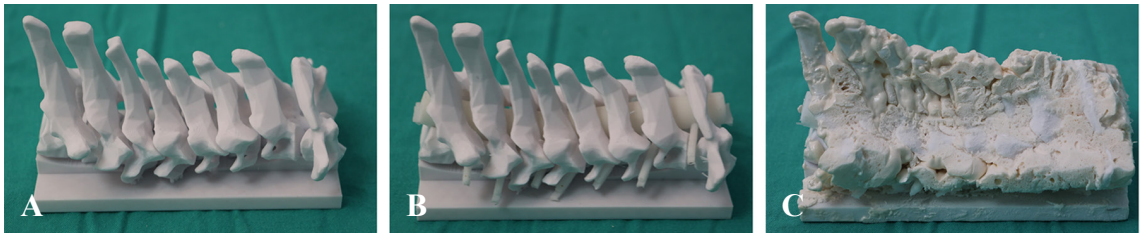

Fig. 1. Three-dimensional (3D) printed cervical spine model assembly stages. **(A)** The raw 3D-printed C1–T1 vertebral model immediately after printing. **(B)** The model after placement of the silicone-based spinal cord and nerve roots; the yellow arrow indicates one of the nerve roots. **(C)** The final state after applying and trimming polyurethane foam, simulating soft tissue and ligamentum flavum.

Fig. 2. The training model housing and setup. **(A)** The dark chamber with sliding mechanism (yellow arrow) and removable lid with gasket (red arrow). **(B)** View showing the cervical spine model being inserted into the sliding track of the chamber. **(C)** The complete setup in surgical configuration, showing the slit openings for instrument access (magenta arrow) and the endoscope with custom handle (green arrow).

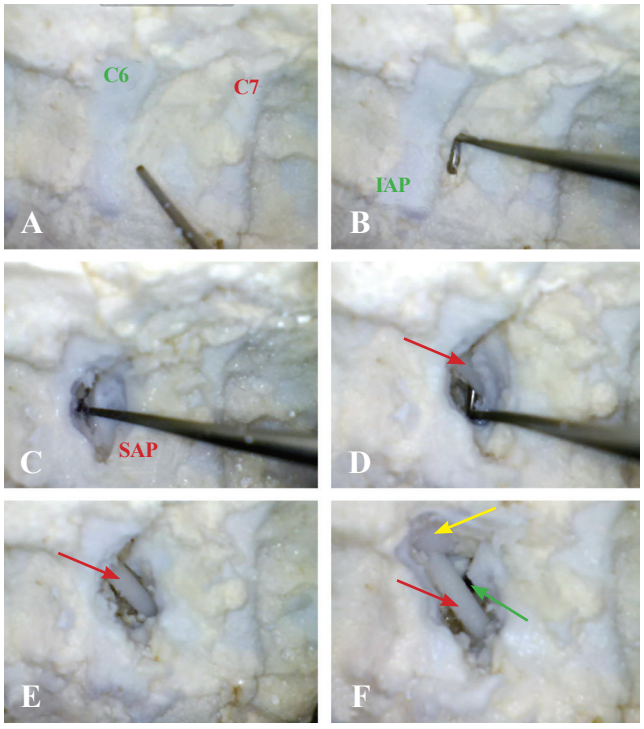

Fig. 3. Endoscopic views captured using the low-cost plumbing endoscope, demonstrating sufficient image quality for training purposes. **(A)** Endoscopic view showing C6 vertebra (green dashed line) and C7 vertebra (red dashed line) with K-wire placement at the facet joint for level localization. **(B)** Surgical hook probing the soft tissue to identify the inferior articular process (IAP) of C6 (outlined in green). **(C)** Visualization after IAP removal reveals the superior articular process (SAP) of C7 (red dashed line) with hook placement for soft tissue mobilization. **(D)** Initial nerve root exposure (red arrow) following partial drilling of the SAP and removal of overlying soft tissue. **(E)** Progressive exposure of the nerve root (red arrow) after additional SAP removal. **(F)** Completed foraminotomy showing the fully decompressed nerve root (red arrow), visible spinal cord (yellow arrow), and exposed disc space (green arrow).

a low-cost plumbing endoscope (Kebidumei, China) was used for visualization (Fig. 2C). Although the quality of this endoscope may not match that of high-end medical equipment, it provided sufficient surgical view for our training purposes and allowed us to keep the overall cost of the model low (Fig. 3). We created a custom polyethylene terephthalate glycol (PETG) handle to house the endoscope and incorporate an irrigation channel compatible with standard intravenous line tubing. Initial trials using a uniportal endoscope design proved unfeasible considering that vibrations from the drill impaired visualization and the specialized surgical tools necessary for that approach were unavailable.

Each newly printed model required approximately 4 hours to print, providing four surgical levels (C3–4, C4–5, C5–6, and C6–7). To account for silicone curing and polyurethane foam setting time, each model required roughly 2 days to prepare and assemble. Switching among residents during the training sessions required less than 5 minutes.

Subject selection and procedure randomization

Residents in their second postgraduate year (PGY 2) were deemed eligible considering that they were capable of taking calls and performing emergency procedures at our clinic. Consequently, eight residents each with over 2 years of training participated in this study. Although all residents were able to perform posterior cervical foraminotomy under supervision, none had previously performed or assisted in endoscopy-assisted posterior cervical foraminotomy. All participating residents were right-handed.

The order of procedures was randomized using the Fisher-Yates shuffle algorithm implemented through the NumPy random.permutation() function (Python ver. 3.x [https://www.python.org/] and NumPy ver. 1.21.0 [https://numpy.org/]) to ensure an unbiased distribution of vertebral levels and operative sides [23,24]. Randomization was organized into blocks of four sessions, each containing two distinct cervical levels and two different sides, thereby standardizing the training intervals and exposure to technique variations.

Training session design

All training sessions were conducted after working hours (18:00 to 20:00) to minimize disruptions and

maintain consistency. The hands-on testing component consisted of three sessions at 1-week intervals to reduce learning decay while allowing adequate rest between sessions. Before the first session, each resident participated in a standardized 30-minute orientation covering the relevant cervical anatomy and radiology in relation to the structures in our 3D-printed model. A pre-operated model was then shown in both plain view and under endoscopic visualization to familiarize the trainees with the silicone nerve roots, simulated dura, polyurethane-based foraminal tissues, and PETG bone structures. This orientation was followed by a 10-minute hands-on exploration, during which the residents practiced manipulating the Midas Rex drill (Medtronic, Dublin, Ireland), Kerrison rongeurs, disc forceps, and a blunt nerve hook under endoscopic guidance.

Once confident with manipulating the endoscope, the residents began the procedure by palpating the spinous processes (starting from C7) to identify the correct level. A Kirschner wire was inserted through the silicone while the research team provided fluoroscopic confirmation (Ziehm Solo fluoroscopy unit; Ziehm Imaging GmbH, Nürnberg, Germany). The attending surgeon recorded the duration from the start of palpation to the final wire placement. The residents were allowed to seek assistance in interpreting the fluoroscopy images or correcting any miscounts of the vertebral levels. Given our emphasis on endoscopic surgical skill rather than fluoroscopic proficiency, necessary help in level identification was provided without penalty.

After confirming the surgical level, the residents introduced the endoscope through the designated opening in the skin overlay, located and removed the Kirschner wire, and then used the Midas Rex drill (Medtronic) to thin the inferior articular process of the superior vertebra and the superior articular process of the inferior vertebra following established protocols. At this step, irrigation was performed using a saline bag connected to the irrigation channel of the endoscope. Once the eggshell thickness of the bone was reached, the residents palpated the space with a blunt hook, mobilized any remaining soft tissue, and removed the bone with 2-mm Kerrison rongeurs to enlarge the surgical corridor. The polyurethane foam meant to mimic the ligamentum flavum was dissected and removed using punch forceps. The trainees concluded the surgery once they believed sufficient bone was removed and the root was fully decompressed, making user to confirm that the hook could be inserted comfortably into the neural foramen and that the margins of the pedicles could be palpated.

Following each session, the attending surgeon reviewed the model in the endoscopic view and then examined the model outside the dark chamber with the trainee, offering visual and tactile feedback on bone removal adequacy and overall technique. Residents also completed a Likert scale questionnaire to evaluate the model's educational value.

Assessment of the surgery

Operative times, the number of fluoroscopic checks, and the duration of fluoroscopy use were documented. Operative time was analyzed separately from fluoroscopic time. Decompression was deemed successful if less than 50% of the facet joint was removed, the nerve root was fully mobilized, a nerve hook could pass smoothly through the foramen, and the margins of the pedicles could be palpated. Excessive bone removal (over 50% of the facet) and root injury (e.g., transection or avulsion) were also recorded. These four key parameters, namely excessive bone removal, root injury, wrong-level surgery, and incomplete decompression, were aggregated into a 4-point score, with 0 signifying a perfect score and 4 representing the most severe outcome.

During Kirschner wire placement, the research team provided radiological assistance to ensure that the correct level was targeted. However, if a resident ultimately performed the procedure on an unintended level (e.g., operating at C5–6 left instead of the planned C4–5 left), the session was documented according to the actual level treated. The originally intended level was then reassigned to a future session, ensuring that each resident still gained experience at every designated level.

Statistical analysis

Analyses were conducted using R software ver. 4.4.2 (R Foundation for Statistical Computing, Vienna, Austria) and IBM SPSS ver. 27.0 (IBM Corp., Armonk, NY, USA). Descriptive statistics were calculated in SPSS, with the results being presented as means and standard deviations for normally distributed variables and medians and interquartile ranges for variables not following normal distributions. For all analyses, statistical significance was set at $p<0.05$.

Our primary statistical approach involved the Brunner-Langer nonparametric analysis (F1-LD model), implemented through the nparLD package in R. This method is particularly well-suited for our study design given that it handles longitudinal data without requiring assumptions of normality or sphericity, making it ideal for small-sample, repeated-measures designs.

We calculated the relative treatment effects (RTEs) for each outcome measure to quantify the magnitude and direction of changes across sessions, with values ranging from 0 to 1, where 0.5 represents no effect. Notably, values above 0.5 indicate higher ranks (generally poorer performance), whereas those below 0.5 indicate lower ranks (typically better performance) relative to the overall distribution of measurements.

Results

Eight neurosurgical residents (five PGY-3, one PGY-4, and two PGY-5) performed a total of 64 procedures, with each resident completing surgeries on all cervical levels from C3–4 to C6–7 distributed equally between the right and left sides.

The most striking finding was the marked disparity in insufficient decompression rates between the sides, with left-sided procedures showing significantly higher rates than did right-sided procedures (25.0% versus 3.6%, p=0.002). Although right-sided procedures tended to have better outcomes than did left-sided procedures, with 57.1% and 35.7% of right- and left-sided procedures having no complications, this difference in overall complication rates did not reach statistical significance (p=0.073).

Surgical metrics showed remarkable consistency across several parameters. No significant differences in operative duration (right: 15:58±9:50 minutes versus left: 13:46±7:47 minutes, p=0.358) or fluoroscopy timing (right: 1:20±0:55 minutes versus left: 1:35±1:04 minutes, p=0.348) were observed between the sides. The number of fluoroscopic images required was also similar between the sides (right: 1.89±1.77 versus left: 2.61±3.51, p=0.341).

Analysis according to cervical level revealed no significant differences in surgical parameters or outcomes. The mean operative times were comparable across all levels (C3–4: 14:25±8:25 minutes; C4–5: 15:14±8:04 minutes; C5–6: 13:35±9:12 minutes; and C6–7: 14:45±9:36 minutes; p=0.961). Similarly, the fluoroscopy requirements showed no level-specific variations in either duration (p=0.977) or number of images (p=0.979). Complication rates, including insufficient decompression (p=0.487), were consistent across all cervical levels.

Time to fluoroscopy improved across sessions, although with marginal statistical significance (analysis of variance [ANOVA]-type test statistic=2.83, degrees of freedom [df]=3.30, p=0.057). The RTEs demonstrated inconsistent patterns of improvement, with some early sessions showing higher values (Time1: RTE=0.70; Time3: RTE=0.73) compared to later sessions (Time4: RTE=0.33; Time8: RTE=0.35) (Fig. 4).

Operative duration significantly improved across sessions (ANOVA-type test statistic=5.99, df=3.10, p=0.004). The initial sessions had notably higher RTEs (Time1: RTE=0.81), with a marked and consistent de-

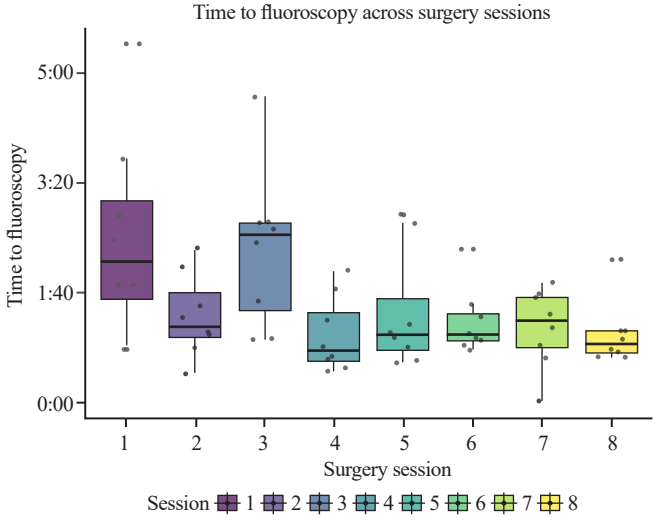

Fig. 4. Box plot showing the time (in minutes) taken to achieve correct fluoroscopic localization across eight surgical sessions. Each point represents an individual procedure, with box plots displaying each session's median, quartiles, and range. The gradual color transition from purple to yellow represents the progression of sessions from 1 to 8. A trend toward decreased fluoroscopy time is observed across successive sessions, with median times decreasing from approximately 2 minutes in early sessions to under 1 minute in later sessions, though with notable variability between procedures.

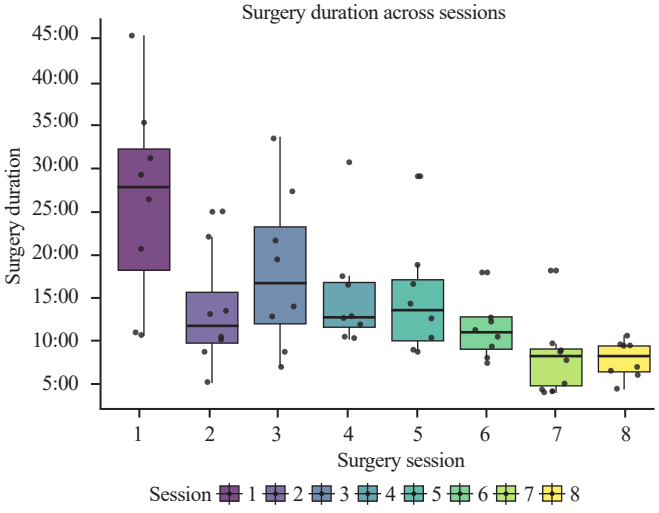

Fig. 5. Box plot demonstrating the progressive reduction in surgical duration (in minutes) across eight training sessions. Each data point represents an individual procedure, with box plots showing each session's median, quartiles, and range. The color gradient from purple (session 1) to yellow (session 8) tracks the chronological progression. A clear trend of decreasing operative times is observed, with median durations reducing from approximately 28 minutes in session 1 to under 10 minutes by session 8 (p=0.004), indicating significant improvement in surgical efficiency with practice.

 https://doi.org/10.31616/asj.2025.0050

crease observed in later sessions (Time7: RTE=0.23; Time8: RTE=0.22) (Figs. 5, 6).

Significant changes in total complications were observed across sessions (ANOVA-type test statistic=4.74, df=3.52, p=0.007). RTE revealed a substantial decrease in complications from early sessions (Time1: RTE=0.77) to later sessions (Time7 and Time8: both RTE=0.26) (Fig. 7).

The number of fluoroscopy images tended to improve, though not reaching statistical significance (ANOVA-type test statistic=2.36, df=3.54, p=0.088). Early sessions required more imaging (Time1–3: RTEs approximately 0.62–0.63), whereas later sessions showed reduced reliance on fluoroscopy (Time8: RTE=0.35).

Resident feedback demonstrated high satisfaction with the educational value of the model, particularly regarding improvements in surgical technique and overall confidence in endoscopic procedures (Fig. 8). However, the participants consistently noted that the low-cost plumbing endoscope used in the study presented some practical challenges, specifically poor image quality and

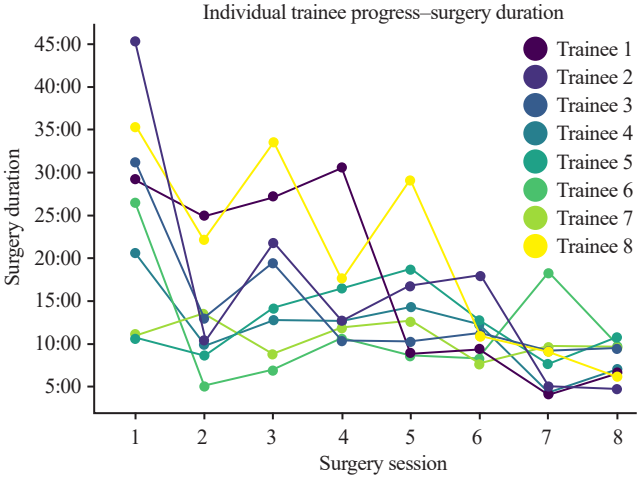

Fig. 6. Line graph showing individual learning curves for each trainee's surgical duration (in minutes) across eight sessions. Each colored line represents a different trainee's progression. While initial performance varied considerably (ranging from approximately 10 to 45 minutes), all trainees demonstrated substantial improvement and converged toward more consistent, shorter operative times (5–10 minutes) by the final sessions, suggesting successful skill acquisition regardless of starting performance.

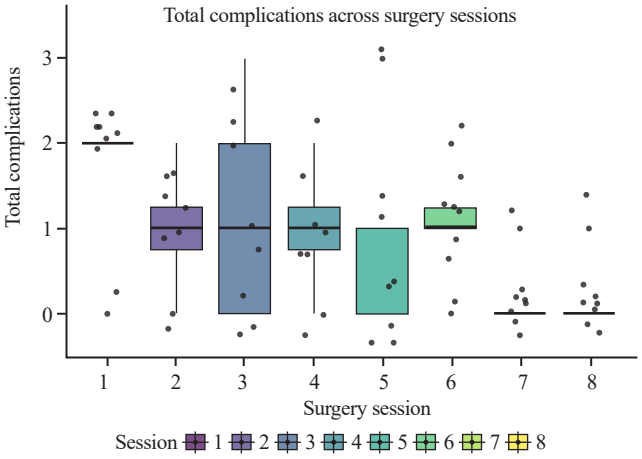

Fig. 7. Box plot depicting the total number of complications per procedure across eight training sessions. Each point represents an individual procedure, with box plots showing the median, quartiles, and range. A significant reduction in complications is observed from early sessions (median of 2 complications) to later sessions (median of 0 complications) (p=0.007). The color progression from purple to yellow represents chronological session order, with later sessions showing lower median values and reduced variability in complication rates.

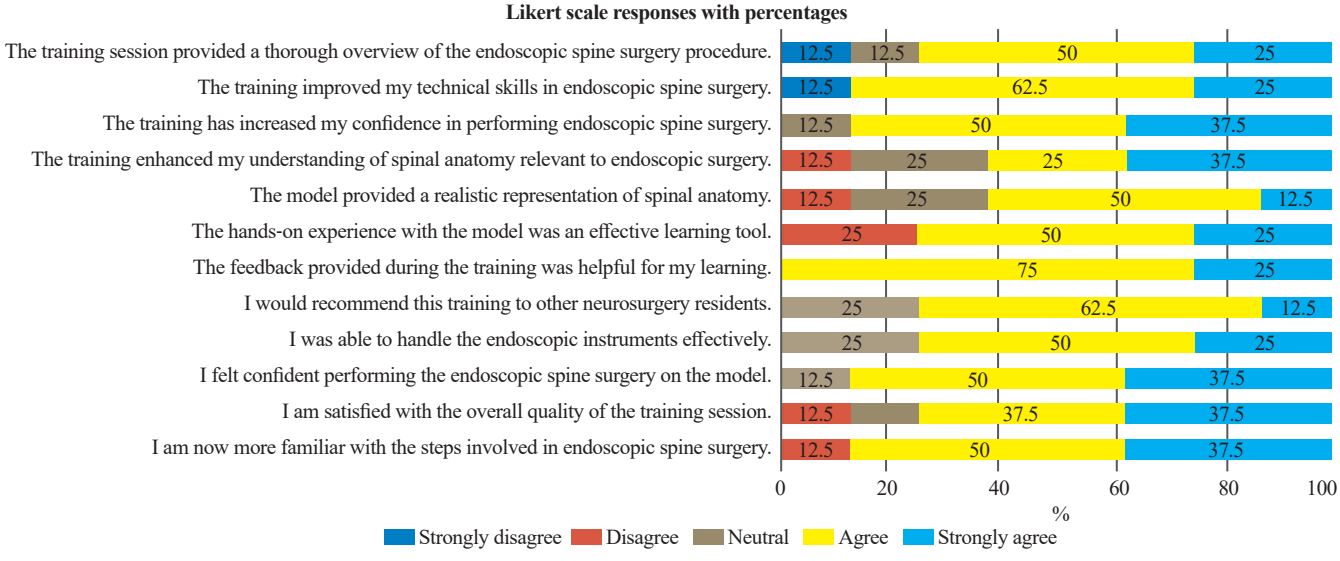

Fig. 8. This figure presents the distribution of responses from trainees (n=8) to a 12-item Likert-scale questionnaire evaluating the training. Each horizontal bar represents a single survey question, with the five response options displayed as stacked segments. The percentages corresponding to each category are shown on the bars.

frequent lens fogging that required periodic cleaning with a gauze. Despite these technical limitations, an intentional trade-off to maintain the model's affordability, the residents still regarded the training experience as highly beneficial for developing fundamental surgical skills (detailed feedback data available in the Supplement 1).

Discussion

The current study assessed the effectiveness of a novel, cost-effective 3D-printed cervical spine model for endoscopic posterior cervical foraminotomy training. Our findings demonstrate that this model reduces operative time and complication rates and provides a safe, controlled environment for residents to hone their skills. This model, similar to the endoscopic lumbar surgery simulator developed in our previous research [22], stands out for its accessibility and affordability.

One of the primary advantages of our model is its low material cost, which had been achieved by using widely available PETG filament, polyurethane foam, and silicone to replicate essential anatomical features at a fraction of the expense associated with traditional simulators or cadaveric training. This significant cost reduction is particularly beneficial for low-resource settings where economic barriers often limit access to advanced surgical education [11,13]. By releasing the model's design and printing guidelines online, we are democratizing neurosurgical education, ensuring that any institution equipped with a standard 3D printer can reproduce our cervical spine simulator. This open-source principle ensures that the benefits of our model, namely its affordability, accessibility, and educational impact, can be broadly shared rather than restricted to high-cost commercial solutions.

An itemized examination of material usage underscores the economic feasibility of our model. The dark box, molds, and handle collectively require around 1,000 g of PETG filament at $17.14/kg (approximately $17.14 in total) and are reusable across multiple sessions. The main silicone "skin" (600 g at $10.97/kg) costs around $6.58 and is also reusable for several training cycles. In contrast, the truly single-use components include the silicone cord (20 g at $0.22 each), the PETG-printed cervical model (85 g at $1.46 each), and the polyurethane foam (60 g at $0.36 per application). These consumables cost approximately $2.04 per new model, providing eight cervical training levels at roughly $0.26 per surgical level. This one-time architecture and low-cost consumables maximize affordability while preserving the tactile and visual realism that novice surgeons require for endoscopic posterior cervical foraminotomy. Although the initial purchase of a 3D printer can be a notable expense, with our study utilizing a Bambu Lab P1S ($800), the same models can also be reliably produced on more budget-friendly devices, such as the Creality Ender-3 S1 ($175).

Aside from its cost-effectiveness, our model aligns with the ethical standards in surgical education. We address the moral complexities and logistical constraints of traditional training methods by offering a realistic simulator that does not require animal or human cadaveric specimens [12,25,26]. Our 3D-printed model provides a practical and ethically sound alternative to animal models and cadaveric studies, which often face sourcing, preservation, and ethical consent issues. Moreover, unlike many augmented or VR platforms [14-18], which can be prohibitively expensive and usually lack robust haptic feedback, our tangible model enables hands-on practice of drilling, nerve retraction, and foraminotomy in a setting that closely mimics real surgical conditions.

A notable finding of our study was the marked disparity in decompression adequacy between surgical sides, with left-sided procedures showing significantly higher rates of insufficient decompression than did right-sided procedures (31.3% versus 3.1%, p=0.003). This laterality effect may be attributed to two factors. First, the posterior–inferior trajectory required for left-sided bone removal with the Kerrison rongeur creates an awkward working angle for right-handed surgeons, potentially compromising the precision and extent of decompression. Second, visualization of the ipsilateral surgical field demands an unintuitive hand position, similar to the challenges in identifying residual disc material during anterior cervical discectomy and fusion procedures. Although our literature review identified only one retrospective single-surgeon series that reported no significant differences between sides [27], our findings suggest that side-specific technical challenges may be particularly relevant during the learning phase of endoscopic procedures. Several strategies could mitigate these laterality-related challenges. Integrating surgical navigation systems early during training could provide real-time feedback on instrument positioning and decompression adequacy. Alternatively, modifying the operative approach by positioning the surgeon on the right side of the patient during the surgical treatment of left-sided pathology might create more ergonomic working angles. Moreover, incorporating downward-cutting Kerrison rongeurs, rather than solely

relying on standard upward-cutting instruments, could improve instrument handling during left-sided procedures. Future research should systematically evaluate these potential solutions, particularly by analyzing early outcomes from experienced training centers, to determine whether this laterality effect persists beyond the learning curve or can be effectively addressed through specific technical modifications.

Similar to our lumbar endoscopy model and previously published models, the current model cannot simulate certain complexities of live surgery, such as active bleeding, muscle tissue, and dynamic tissue responses [19,22,28,29]. Likewise, the model fails to accommodate all potential anatomical variability or fully simulate water inflow or the nuanced sensation of human bone under a high-speed drill. Hence, despite being an invaluable stepping stone, the simulator should be complemented by higher-fidelity training modalities, such as cadaver labs, advanced VR systems, or ultimately supervised live surgeries.

Another area for improvement is the sample size and generalizability of our study. As with any pilot study, our participant pool was limited to a modest number of residents affiliated with a single institution. Although our power analysis and effect sizes indicated robust improvements in operative times, future research should involve larger cohorts and diverse training environments to better capture variability in skill acquisition and affirm our findings' external validity. Furthermore, despite having tracked parameters such as fluoroscopy use and operative times, objective measures of complication risk, especially dural tears or nerve root injuries, remain challenging to simulate. This shortcoming underscores the need for continued research and development in surgical simulation.

Another vital consideration for simulating iatrogenic trauma is the choice of the soft-tissue analog. Our lumbar discectomy model used thermoplastic polyurethane (TPU) filaments for the dura and nerve roots, allowing the paint layers to peel off with tool mismanagement and reveal the extent of damage [22]. For the cervical model, we opted for silicone to more faithfully replicate the cord and root structures. In thin, delicate segments (roots with a diameter of 3 mm), silicone more closely approximates the elasticity and tactile sensation of the cervical anatomy than does TPU. However, silicone is famously nonadhesive, consequently preventing the application of the paint layers designed to peel and reveal microtrauma, as had been done previously. In practice, however, the smooth surface of silicone makes cuts and defects visually obvious, reducing the need for paint layers. Regardless, the lack of a paint-peel metric hinders the precise quantification of minor surface abrasions. Future refinements could explore other forms of surface treatments to more systematically simulate dural or nerve injury.

Despite these constraints, the model offers an innovative, replicable framework for initial training in endoscopic posterior cervical foraminotomy. Participants found the simulator realistic enough to build confidence in surgical ergonomics, drill handling, and endoscopic visualization, skills that can be transferable to higher-fidelity training or clinical practice once established. From an institutional standpoint, the low cost and ease of printing make our model suitable for repeated, iterative practice sessions. This architecture is particularly beneficial for novice residents who often require extended hands-on exposure before developing proficiency in delicate endoscopic procedures.

Our 3D-printed model also has substantial potential for expansion beyond its current application. The system could be readily adapted for more complex procedures, such as cervical decompression or laminoplasty, by maintaining the same baseplate and dark chamber structure. One promising avenue involves incorporating patient-specific anatomical variations by converting DICOM images from real patients with foraminal or central stenosis into printable 3D models and integrating these into our baseplate design, a process that typically requires less than a day to complete. To further democratize neurosurgical education, these models could utilize anonymized cases from open repositories, such as the DICOM Library, funded by the European Union, allowing free sharing across training institutions worldwide. Integration into augmented reality represents another compelling frontier, enabling trainees to visualize tool and camera positioning in real-time when combined with navigation systems. Such a technology could enhance spatial awareness during procedures or more comprehensively simulate the operating room environment. Although these advanced applications exceed the current scope of our study, they offer perspectives for future collaborative research efforts aimed at further reducing barriers to high-quality endoscopic spine surgery training.

Conclusions

Our 3D-printed cervical spine simulator represents another step toward our broader initiative to democratize neurosurgical education. Much like our previously reported model for lumbar endoscopic surgery, this cer-

vical platform underscores the feasibility of combining open-source 3D printing technology, inexpensive materials, and carefully engineered designs to produce a practical training solution. Although our model cannot simulate the complexity and variability of live surgery, it is a powerful adjunct for bridging the gap between theoretical knowledge and high-fidelity surgical practice, ultimately enhancing the confidence and competence of neurosurgery trainees.

Key Points

- The materials needed to construct this innovative three-dimensional-printed spine model cost less than $1 per training level, making it highly affordable.
- The use of the model significantly improved surgical efficiency, with mean operative durations decreasing from 21:42±2:15 to 6:33±0:42 minutes across training sessions.
- The model effectively simulates tissue handling using silicone-based neural elements, polyurethane foam-based ligaments, and polyethylene terephthalate glycol vertebrae, providing residents with realistic tactile feedback.
- This accessible and cost-effective alternative to cadaveric training significantly reduced complication rates across sessions (from 2.1±0.8 to 0.4±0.5), making it suitable for various resource settings.

Conflict of Interest

No potential conflict of interest relevant to this article was reported.

Acknowledgments

The data supporting this study's findings are available in the supplementary files.

Funding

This work was funded by the Ege University Office of Scientific Research Projects (Project number: 32406).

ORCID

Bilal Bahadır Akbulut: https://orcid.org/0000-0002-7983-5056;
Elif Ezgi Çenberlitaş: https://orcid.org/0009-0004-2363-6885;
Mustafa Serdar Bölük: https://orcid.org/0000-0002-9406-4114;
Taşkın Yurtseven: https://orcid.org/0000-0001-7982-8115;
Hüseyin Biçeroğlu: https://orcid.org/0000-0003-2306-0826

Author Contributions

Conceptualization: HB, TY. Data curation: BBA, EEC. Formal analysis: BBA, MSB. Funding acquisition: BBA. Investigation: BBA, EEC, MSB. Methodology: BBA, EEC, MSB. Project administration: HB, TY. Resources: BBA, MSB. Software: BBA. Supervision: HB, TY. Validation: HB, TY. Visualization: BBA. Writing–original draft: BBA, EEC, MSB. Writing–review and editing: HB, TY. Final approval of the manuscript: all authors.

Supplementary Materials

Supplementary materials can be available from https://doi.org/10.31616/2025.0050. Supplement 1. Likert scale questionnaire answers of the residents and their surgery data.

References

1. Oertel JM, Philipps M, Burkhardt BW. Endoscopic posterior cervical foraminotomy as a treatment for osseous foraminal stenosis. World Neurosurg 2016;91:50-7.
2. Zhang C, Wu J, Xu C, et al. Minimally invasive full-endoscopic posterior cervical foraminotomy assisted by O-arm-based navigation. Pain Physician 2018;21:E215-23.
3. Gatam AR, Gatam L, Phedy, et al. Full endoscopic posterior cervical foraminotomy in management of foraminal disc herniation and foraminal stenosis. Orthop Res Rev 2022;14:1-7.
4. Wu PF, Liu BH, Wang B, et al. Complications of full-endoscopic versus microendoscopic foraminotomy for cervical radiculopathy: a systematic review and meta-analysis. World Neurosurg 2018;114:217-27.
5. Ruetten S, Komp M, Merk H, Godolias G. Full-endoscopic cervical posterior foraminotomy for the operation of lateral disc herniations using 5.9-mm endoscopes: a prospective, randomized, controlled study. Spine (Phila Pa 1976) 2008;33:940-8.
6. Kim YR, Kim JH, Park TH, et al. Overview and prevention of complications during full-endoscopic cervical spine surgery. J Minim Invasive Spine Surg Tech 2023;8:153-64.
7. Ju CI, Kim P, Seo JH, Kim SW, Lee SM. Complications of cervical endoscopic spinal surgery: a systematic review and narrative analysis. World Neurosurg 2023;178:330-9.
8. Olson TE, Upfill-Brown A, Park DY. Endoscopic posterior cervical foraminotomy techniques and outcomes. Semin Spine Surg 2024;36:101086.
9. Lee SH, Seo J, Jeong D, et al. Clinical outcomes and compli-

cations of unilateral biportal endoscopic posterior cervical foraminotomy: a systematic review and meta-analysis with a comparison to full-endoscopic posterior cervical foraminotomy. Neurospine 2024;21:807-19.
10. Ransom NA, Gollogly S, Lewandrowski KU, Yeung A. Navigating the learning curve of spinal endoscopy as an established traditionally trained spine surgeon. J Spine Surg 2020;6(Suppl 1):S197-207.
11. Grimes CE, Bowman KG, Dodgion CM, Lavy CB. Systematic review of barriers to surgical care in low-income and middle-income countries. World J Surg 2011;35:941-50.
12. Reuters. The body trade: cashing in on the donated dead [Internet]. London: Reuters; 2017 [cited 2025 Jan 18]. Available from: http://www.reuters.com/investigates/section/usa-bodies/
13. Wilkinson E, Aruparayil N, Gnanaraj J, Brown J, Jayne D. Barriers to training in laparoscopic surgery in low- and middle-income countries: a systematic review. Trop Doct 2021;51:408-14.
14. Amini A, Allgaier M, Saalfeld S, et al. Virtual reality vs phantom model: benefits and drawbacks of simulation training in neurosurgery. Oper Neurosurg (Hagerstown) 2024;27:618-31.
15. Zaki MM, Joshi RS, Joseph JR, et al. Virtual reality-enabled resident education of lateral-access spine surgery. World Neurosurg 2024;183:e401-7.
16. Alaraj A, Charbel FT, Birk D, et al. Role of cranial and spinal virtual and augmented reality simulation using immersive touch modules in neurosurgical training. Neurosurgery 2013;72 Suppl 1:115-23.
17. Mishra R, Narayanan MD, Umana GE, Montemurro N, Chaurasia B, Deora H. Virtual reality in neurosurgery: beyond neurosurgical planning. Int J Environ Res Public Health 2022;19:1719.
18. Akgun MY, Baran O, Ogretmen E, et al. Use of 3- dimensional modeling and virtual reality in the education of posterior spinal instrumentation. Turk Neurosurg 2024;34:958-65.
19. Park HJ, Wang C, Choi KH, Kim HN. Use of a life-size three-dimensional-printed spine model for pedicle screw instrumentation training. J Orthop Surg Res 2018;13:86.
20. Koh JC, Jang YK, Seong H, Lee KH, Jun S, Choi JB. Creation of a three-dimensional printed spine model for training in pain procedures. J Int Med Res 2021;49:3000605211053281.
21. BodyParts3D/Anatomography: select parts and make embeddable model of your own [Internet]. Tokyo: BodyParts3D/Anatomography [date unknown] [cited 2025 Jan 13]. Available from: https://lifesciencedb.jp/bp3d/
22. Akbulut BB, Boluk MS, Biceroglu H, Yurtseven T. Evaluating the efficacy of a cost-effective, fully three-dimensional-printed vertebra model for endoscopic spine surgery training for neurosurgical residents. Asian Spine J 2024;18:630-8.
23. Welcome to Python.org [Internet]. Wilmington (DE): Python Software Foundation; 2025 [cited 2025 Jan 18]. Available from: https://www.python.org/
24. Harris CR, Millman KJ, van der Walt SJ, et al. Array programming with NumPy. Nature 2020;585:357-62.
25. Kovacs G, Levitan R, Sandeski R. Clinical cadavers as a simulation resource for procedural learning. AEM Educ Train 2018;2:239-47.
26. Abbasi H, Abbasi A. Using porcine cadavers as an alternative to human cadavers for teaching minimally invasive spinal fusion: proof of concept and anatomical comparison. Cureus 2019;11:e6158.
27. Foocharoen T. Biportal endoscopic spine surgery for single lumbar disc herniation or lumbar stenosis: comparison between right and left side approach of right-handed surgeon. J Southeast Asian Orthop 2020;44:11-8.
28. Li Y, Li Z, Ammanuel S, Gillan D, Shah V. Efficacy of using a 3D printed lumbosacral spine phantom in improving trainee proficiency and confidence in CT-guided spine procedures. 3D Print Med 2018;4:7.
29. Clifton W, Damon A, Stein R, Pichelmann M, Nottmeier E. Biomimetic 3-dimensional-printed posterior cervical laminectomy and fusion simulation: advancements in education tools for trainee instruction. World Neurosurg 2020;135:308.